Modeling of Single Mode Optical Fiber having a Complicated Refractive Index Profile by using Modified Scalar Finite Element Method

[1]Sanjeev Kumar Raghuwanshi and [2]B. M. Azizur Rahman

[1,2]Instrumentation and Sensor Division, School of Engineering and Mathematical Sciences, Northampton Square, City University London, EC1 V 0HB, UK

[1]Corresponding Author: sanjeevrus@yahoo.com

Abstract

A numerical method based on modified scalar finite element method (SC-FEM) is presented and programmed on MATLAB platform for optical fiber modeling purpose. We have estimated the dispersion graph, mode cut off condition, and group delay and waveguide dispersion for highly complicated chirped type refractive index profile fiber. The convergence study of our FEM formulation is carried out with respect to the number of division in core. It has been found that the numerical error becomes less than 2 % when the number of divisions in the core is more then 30. To predict the accurate waveguide dispersion characteristics, we need to compute expression $\frac{d^2(Vb)}{dV^2}$ numerically by the FEM method. For that the normalized propagation constant b (in terms of β) should be an accurate enough up to around 6 decimal points. To achieve this target, we have used 1 million sampling points in our FEM simulations. Further to validate our results we have derived the higher order polynomial expression for each case. Comparison with other methods in calculation of normalized propagation constant is found to be satisfactory. In traditional FEM analysis a spurious solution is generated because the functional does not satisfy the boundary conditions in the original waveguide problem, However in our analysis a new term that compensate the missing boundary condition has been added in the functional to eliminate the spurious solutions. Our study will be useful for the analysis of optical fiber having varying refractive index profile.

Keywords: Chirp Type's refractive index profile, waveguide dispersion, group delay, finite element method (FEM)

1. Introduction

In this paper, a modified finite element method (FEM) based on a variational formulation for cylindrical coordinates system, which can consider complicated refractive index profile is presented and results are simulated on MATLAB platform. Like the other numerical methods, the FEMs are widely utilized methods. The SC-FEM presented in this paper has a certain advantages over the vectorial FEM, like SC-FEM has no spurious problem. Due to this facilitation since the matrix size for our analysis is one-third to two-thirds smaller than that for traditional analysis, required memory and CPU time become very small. The result of our computation is well agreed with the previously published results by other methods like vector-FEM, finite difference method, etc.

The optical fibers can be in various structural dissimilarities just like in photonic crystal fiber has various size or shapes of holes. Many critical steps may involve during these type of optical fibers fabrication process [1-5]. The modeling process plays an important role in the development of optical fibers and related devices by evaluating the geometrical design performance such as guiding properties, mode confinement capability to mention few. Optical waveguide modeling techniques can be divided into analytical and numerical methods. Numerical methods are preferred whenever the analytical solution is not possible for certain geometry like in photonic crystal optical fiber. For the numerical methods, several approaches, this includes the scalar or vectorial finite difference method, scalar or vectorial finite element method, and Beam propagation method are preferred. Apart of that a semi-analytical method has also developed to analyze a taper optical waveguide [6-12]. Instead of finite element method, finite difference method may also be preferred in certain cases due to easier formulation procedure; however accumulation of truncation error and long computation time may reduce the method feasibility. In order to overcome these problems in this paper we opted the finite element method analyses in order to produce acceptable simulation results while shorten the time. In case of weakly guiding approximation, we can efficiently use the scalar wave equation solution instead of fully vectorial method for complicated waveguides. Indeed in this paper we use the weakly guiding approximation throughout for all the cases like chirped/alpha power refractive index profile. It then obtained the scalar wave equation by ignoring the terms for the interaction between two polarized field components in the vectorial wave equations. Since in our FEM formulation we are dealing with a single mode fiber with degenerate mode (HE_{11} mode having same polarization state in principal), hence the error generated by scalar FEM while compared to vectorial FEM is negligible [13-31].

2. Finite element method analysis of optical fibers

In this section, variational formulation based on FEM analysis of the HE_{11} mode in optical fibres having a complex refractive-index profile is described. Figure 1 reveals the core region $0 \leq r \leq a$ where the refractive index can be an arbitrary profile. The maximum refractive index of the core is denoted as $n_1 (= 1.5)$ and that in the cladding as $n_0 (= 1.4775)$. The wave equation correspond to HE_{11} mode is given, by with $m = 0$ as [12-14]

$$\frac{\mathbf{1}}{\mathbf{r}}\frac{\mathbf{d}}{\mathbf{dr}}\left(\mathbf{r}\frac{\mathbf{dE}}{\mathbf{dr}}\right) + \left(\mathbf{k^2 n^2 - \beta^2}\right)\mathbf{E} = \mathbf{0} \qquad (\mathbf{1})$$

where E denotes electric field. The boundary condition is given by the continuity for E and dE/dr at $r = a$.

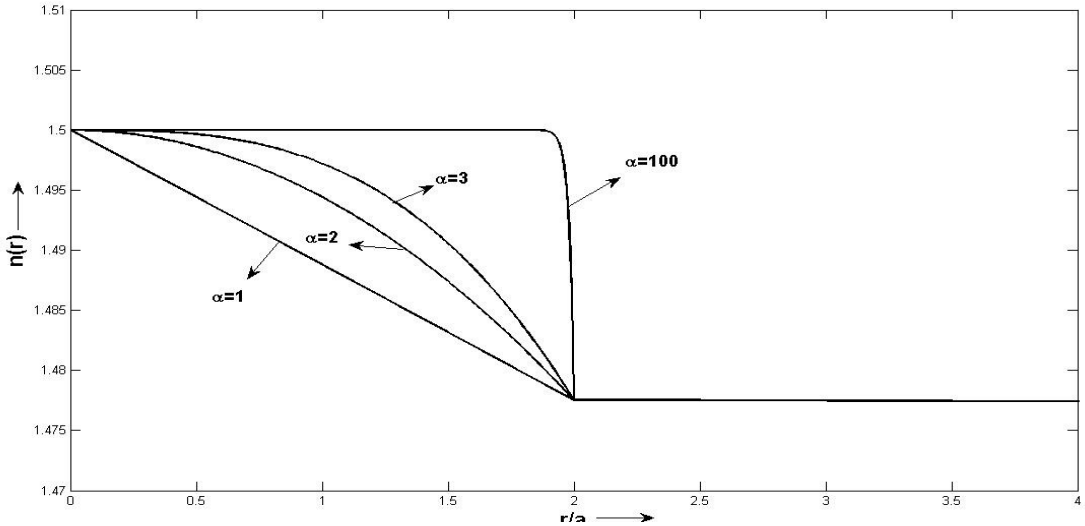

Fig. 1: Refractive-index distribution and schematic of α- power refractive index distribution of inhomogeneous optical fiber, where 'a' is the core radius.

Before transforming eq. (1) into a variation expression, the waveguide parameters are normalized as

$$\boldsymbol{\rho = \frac{r}{a}, E_t(r) = R(a), D = \frac{A}{a}} \qquad (\mathbf{2})$$

where $r = A$ and $\rho = D$ corresponds to the core and cladding interface. Following this normalization, the wave equation and the boundary condition are rewritten as

$$\left.\begin{aligned} &\frac{1}{\rho}\frac{d}{d\rho}\left(\rho\frac{dR}{d\rho}\right) + [\,v^2 q(\rho) - w^2]R = 0, \\ &R(\rho) and \frac{dR(\rho)}{d\rho} are\ continuos\ at\ \rho = D \end{aligned}\right\} \qquad (3)$$

Here the transverse wavenumber w, the normalized frequency v and the normalised refractive index profile $q(\rho)$ are given by

$$\left.\begin{aligned} w &= a^2\sqrt{\beta^2 - k^2 n_0^2} \\ v &= ka\sqrt{(n_1^2 - n_0^2)} \\ q(\rho) &= \frac{n^2 - n_0^2}{n_1^2 - n_0^2} \end{aligned}\right\} \qquad (4)$$

The solution of the wave eq. (3) under the constraint of the boundary condition can be obtained as the solution of the variational problem that makes the functional stationary: as follows [15-25]

$$\boldsymbol{I[R] = -\int_0^x \left(\frac{dR}{d\rho}\right)^2 \rho\, d\rho + \int_0^x \left[v^2 q(\rho) - w^2\right] R^2 \rho d\rho} \qquad (\mathbf{5})$$

The validity of eq. (5) is proved in a similar manner to that in ref [24, 26]. Having to solve the eq. (5) field profile in the core is dicretised and expressed as

$$\boldsymbol{R(\rho)} = \begin{cases} \sum_{\boldsymbol{i=0}}^{\boldsymbol{N}} \boldsymbol{R_i \phi_i(\rho)} & (\boldsymbol{0 \le \rho \le D} \\ \boldsymbol{\frac{R_n}{K_0(wd)} K_0(w\rho)} & (\boldsymbol{\rho > D}) \end{cases} \qquad (\boldsymbol{6})$$

where $R_0 - R_N$ are the field values at the sampling points to be solved and K_0 is 0^{th} order modified Bessel function. Also

$$\left.\begin{aligned} \mathrm{R_i} &= \mathrm{R}(\rho_\mathrm{i}) \quad \text{for } (\mathrm{i} = 0 - \mathrm{N}) \\ \rho_\mathrm{i} &= \mathrm{i}\frac{\mathrm{D}}{\mathrm{N}} \quad \text{for } (\mathrm{i} = 0 - \mathrm{N}) \end{aligned}\right\} \qquad (7)$$

The solutions in the cladding and the substrate are given by the analytical functions. The sampling function $\phi_\mathrm{i}(\rho)$ becomes unity at $\rho = \rho_\mathrm{i}$, becomes zero at the neighboring sampling points $\rho = \rho_{\mathrm{i}-1}$ and $\rho = \rho_{\mathrm{i}+1}$, and is zero throughout all other regions. The precise expressions of $\phi_\mathrm{i}(\rho)$ are given by,

$$\phi_0(\rho) = \begin{cases} \frac{\mathrm{N}}{\mathrm{D}}(\rho_\mathrm{i} - \rho) & 0 \le \rho \le \rho_\mathrm{i} \\ 0 & \text{All other areas} \end{cases} \qquad (8)$$

$$\phi_\mathrm{i}(\rho) = \begin{cases} \frac{\mathrm{N}}{\mathrm{D}}(\rho - \rho_{\mathrm{i}-1}) & (\rho_{\mathrm{i}-1} \le \rho \le \rho_\mathrm{i}) \\ \frac{\mathrm{N}}{\mathrm{D}}(\rho_{\mathrm{i}+1} - \rho) & (\rho_\mathrm{i} \le \rho \le \rho_{\mathrm{i}+1}) \\ 0 & \text{All other areas} \end{cases} \qquad (9)$$

$$\phi_\mathrm{N}(\rho) = \begin{cases} \frac{\mathrm{N}}{\mathrm{D}}(\rho - \rho_{\mathrm{N}-1}) & (\rho_{\mathrm{N}-1} \le \rho \le \rho_\mathrm{N}) \\ 0 & \text{All other areas} \end{cases} \qquad (10)$$

Since the sampling function here is a linear function of ρ, eq. (6) means that the continuous function R(ρ) is approximated by the broken lines. The normalized refractive index distribution q(ρ) is also approximated, by using the sampling function, as

$$\mathrm{q}(\rho) = \sum_{\mathrm{i}=0}^{\mathrm{N}} \mathrm{q_i}\phi_\mathrm{i}(\rho) \qquad (11)$$

$$\mathrm{q_i} = \frac{\mathrm{n}^2(\rho_\mathrm{i}) - \mathrm{n_s^2}}{\mathrm{n_1^2} - \mathrm{n_s^2}} \qquad (12)$$

Substituting eq. (6) in eq (5), we obtain the functional

$$I = -\int_0^D \left(\frac{dR}{d\rho}\right)^2 \rho\, d\rho + \int_0^D [v^2 q(\rho) - w^2] R^2 \rho d\rho - \frac{wDK_1(wD)}{K_0(wD)} R_N^2 \qquad (13)$$

The detail derivation of above eq. (13) is given in Appendix-I ("A.1").

3. Modeling of Graded Types Refractive Index Profile of Single mode Optical fiber

Once the eigenvalue equation for matrix C as described in "Appendix A.2 is solved to find the allowed values of wave propagation constant β leading to obtain the corresponding eigenvector $R_0, R_1, \ldots\ldots\ldots R_N$ by simple matrix operation. Here $R_i (i = 1 - N)$ is obtained with respect to R_0 ($\neq 0$), while R_0 is still yet to find out. The total optical power P has to be normalized to obtain R_0. Figure 1, show the α-power refractive index profiles given by [23, 25], for an optical fiber and planar slab waveguide respectively

$$n^2(r) = \begin{cases} n_1^2 - (n_1^2 - n_0^2)\left(\frac{r}{a}\right)^{\alpha}, (0 \le r \le a) & for\ Fiber \\ n_0^2 \quad (r > a) & \end{cases}$$

$$n^2(x) = \begin{cases} n_s^2 & (x < 0) \\ n_1^2 - (n_1^2 - n_s^2)\left|\frac{x}{a} - 1\right|^{\alpha} & (0 \le x \le 2a) \quad \text{for planar slab} \\ n_s^2 & (x > 2a) \end{cases} \quad (14)$$

The planar slab waveguide is a basic structure through one can design various types of integrated optical waveguide structure. In this paper the objective is to compare the circular core fiber case with planar slab waveguide case. This is because the coordinates are different but the wave equation is same for both the cases [32-34]. Hence the validity of the results can be established better. Next, we shows the results of FEM analyses for HE_{11} of optical fiber while comparing with TE modes of planar slab waveguide in the α-power refractive-index profiles given by eq. (14). We consider the total core radius to be "2a" and the sampling point in the core $N = 100$. The step-index slab waveguide is also analyzed by setting $\alpha = \infty$ in eq. (14). Figure 2 reveals the normalized cut off frequency V_c. It is apparent α tends to be $\alpha \to 100$ correspondingly $V_c \to V_{co} \to 2.405$. To know the accuracy of the computation in our FEM formulation, the percentage of numerical error $(V_c - V_{c0})/V_{c0} \times 100$ (%) for the cut off normalized frequency in case of step index profile (where V_{c0} is the cutoff frequency for step index profile) is computed with respect to the number of core divisions N. Figure 3 reveals the validity of our simulation by the fact that if the number of core division is around 70 the error even become less than 1 %. Figures 4-6 shows the normalized propagation constant b, field vector and propagation constant in terms of β/k for the HE_{11}mode of optical fiber while comparing with TE_0 mode of planar slab waveguides with α-power refractive-index profiles respectively. Here, we assumed $n_1 = 1.5, n_s = n_0 = 1.4775$ and $r = 2a = 2\mu m$ hence $A = 2\mu m$.

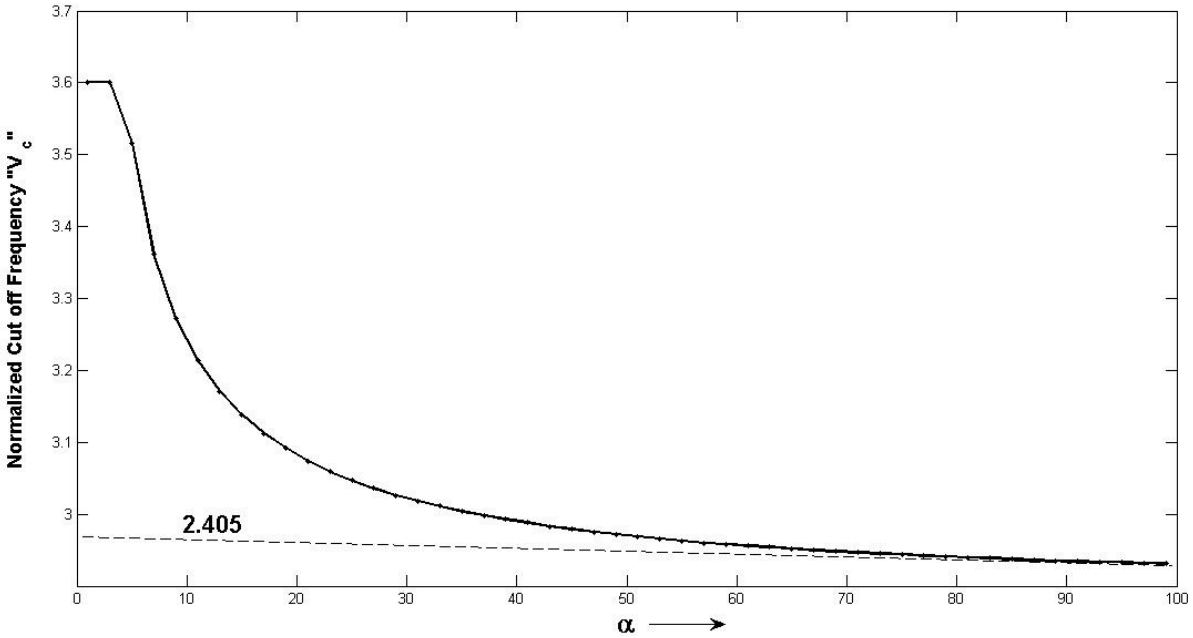

Fig. 2: Cutoff normalized frequency V_c of optical fiber for HE_{11} mode with α-power refractive-index profiles.

From the observation of the Figure 4 , it is apparent that the planar slab waveguide behaves more or less similarly as an optical fiber near cut off frequency (low v-number range of $0 \leq v \leq 1.3$) for any type of profile. However the triangular profile shows much difference in their behvior far from cut off region. We can also conclude that the fundamental mode of an optical fiber HE_{11} behaves in a similar way as TE_{01} mode of planar slab waveguide for step index profile case.

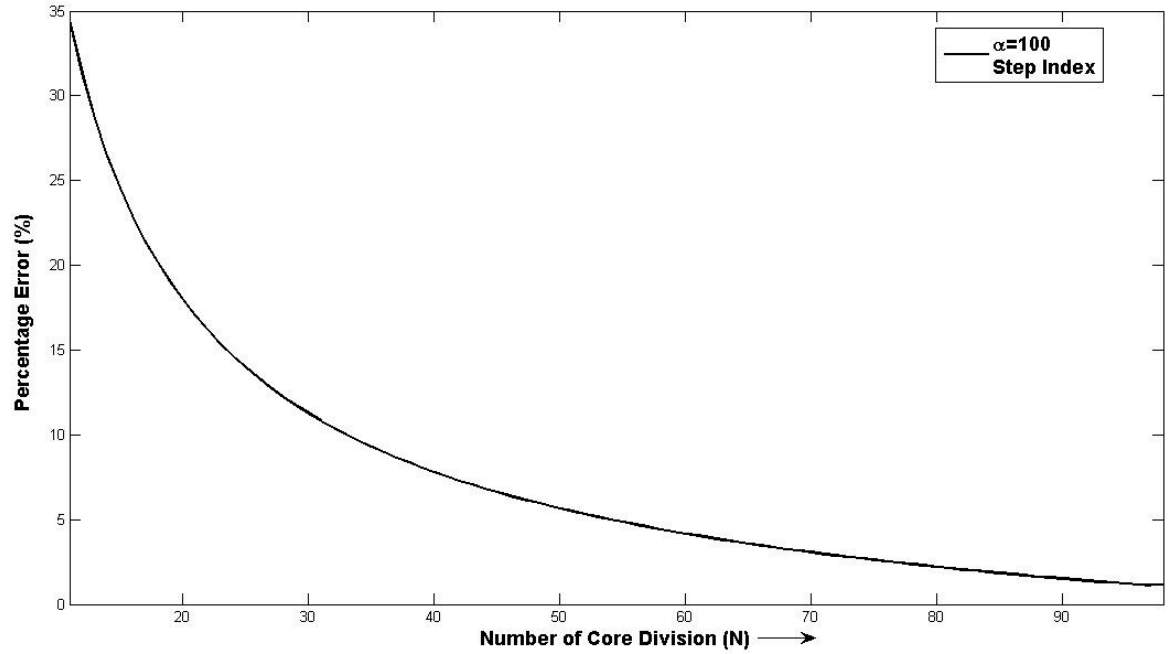

Fig. 3: Percentage error for the cut-off normalized frequency with respect to the number of core divisions N in FEM analysis for step index profile for HE_{11} mode.

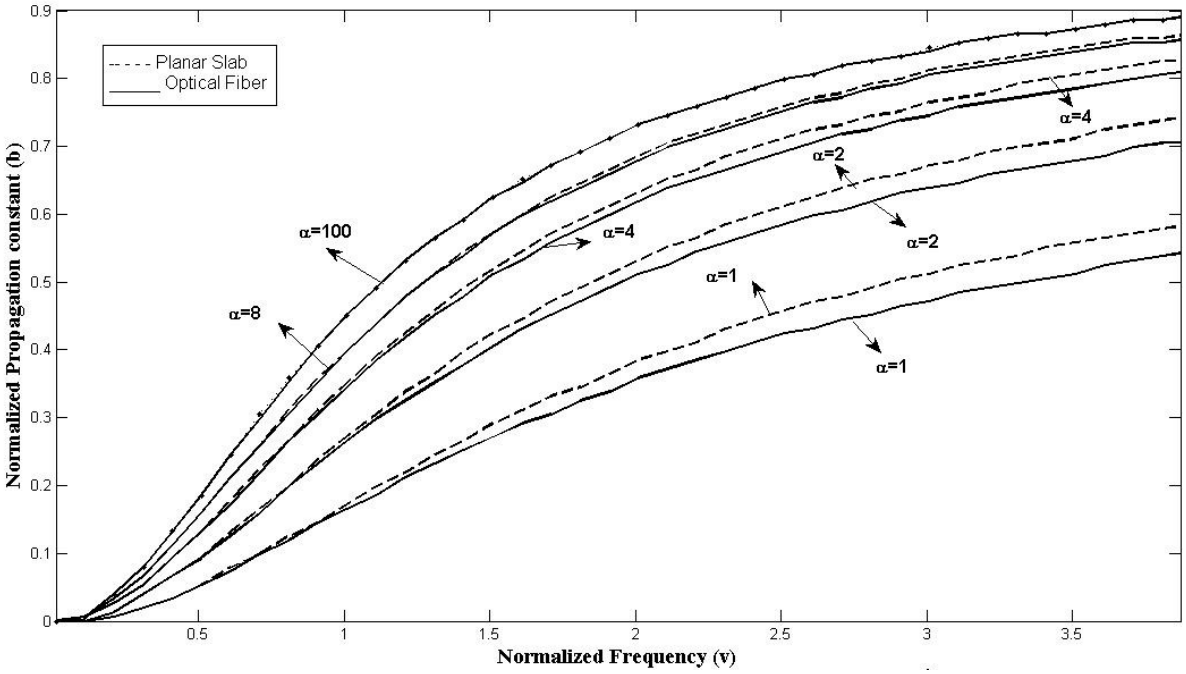

Fig. 4: Normalized propagation constant (b) of optical fiber (HE_{11} mode) and planar slab (TE_{01} mode) waveguides with α-power refractive-index profiles.

Figure 4 also reveals that in case of triangular profile case the power of fundamental mode is more tightly confined in the core region of optical fiber hence these properties can be used for strongly guided fiber applications. Cross sectional view of the electric field E and magnetic field H vectors for the case of HE_{11} is shown in Fig. 5. It is apparent from this plot that E vector is perpendicular to H field vector. The plot of E_x component for the case of HE_{11} mode is shown in Fig. 6. Figures 5 and 6 corresponds to $\mathrm{n}_1 = 1.476, \mathrm{n}_0 = 1.446$ and $r = 3\mu m$ ($A = 3\mu m$ and $a = 1\mu m$) at $\lambda = 1.55\ \mu m$ while computed allowed value of $\beta = 5.9538\ \frac{1}{\mu m}$. Once the propagation constant β is known for entire wavelength of interest to us we can predict the dispersion characteristics of an optical fiber or a waveguide having a complex refractive index profile. After knowing the normalized propagation characteristics we can calculate $\frac{\mathrm{d}(v.b)}{\mathrm{dv}}$ and $\mathrm{v}\frac{\mathrm{d}^2(v.b)}{\mathrm{dv}^2}$ for any type of refractive index profile case. Further we can calculate the waveguide dispersion by using the following expression [23-25],

$$\mathrm{D_W} = -\frac{(\mathrm{n_1} - \mathrm{n_s})}{\mathrm{c}\lambda}\mathrm{v}\frac{\mathrm{d}^2(v.b)}{\mathrm{dv}^2} \tag{15}$$

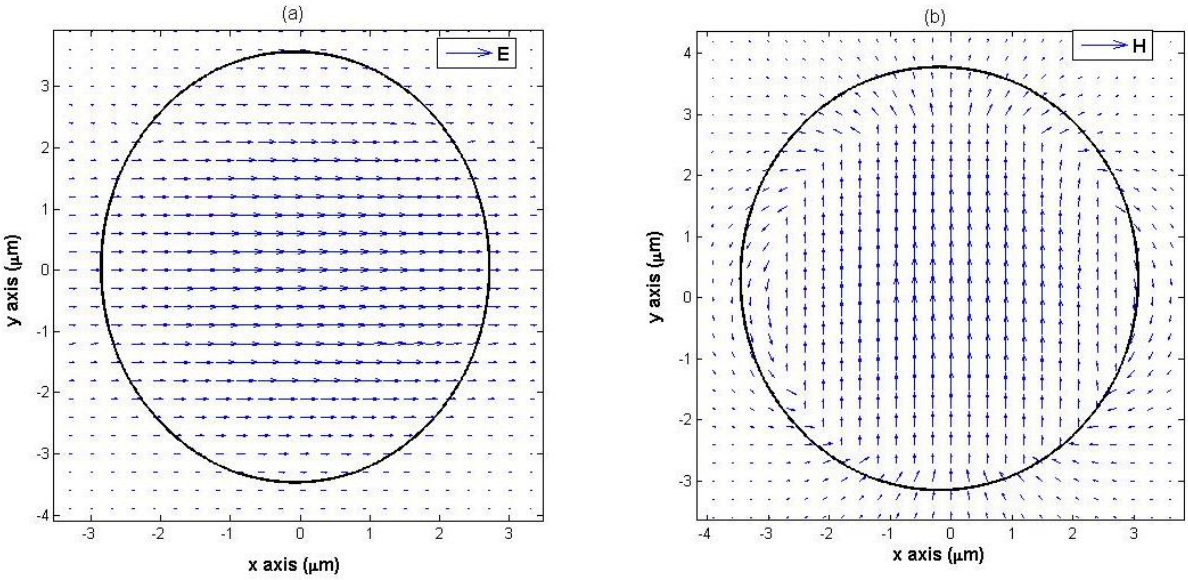

Fig. 5: Cross sectional view of the a) electric field and b) magnetic field vectors for the case of $HE_{11}(\lambda = 1.55\ \mu m)$ mode.

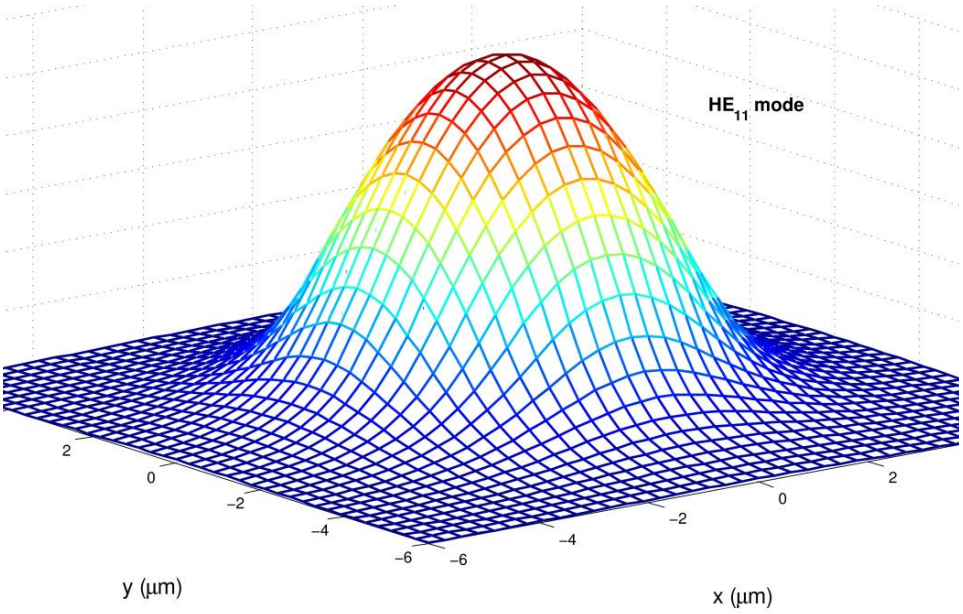

Fig. 6: Plot of electric field vector E_x component for the case of $HE_{11}(\ \lambda = 1.55\ \mu m)$ mode.

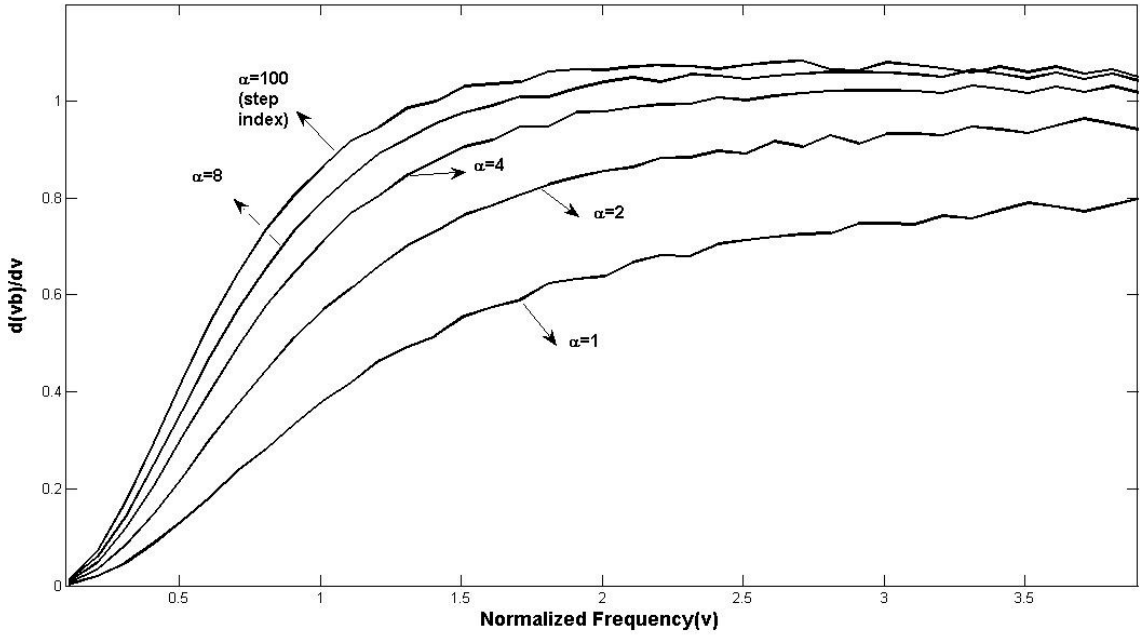

Fig. 7: Normalized delay $\frac{d(Vb)}{dV}$ of optical fiber with α-power refractive index profiles.

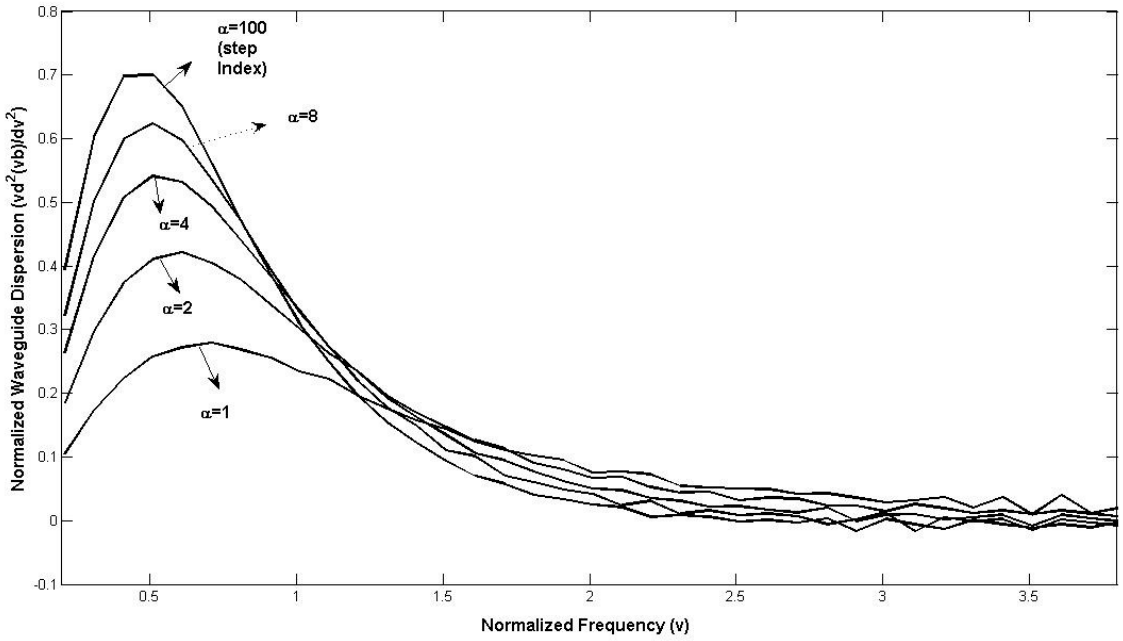

Fig. 8: Normalized waveguide dispersion parameter $v\frac{d^2(Vb)}{dV^2}$ of optical fiber with α-power refractive index profiles.

Figure 7-8 reveals the normalized delay $\frac{d(v.b)}{dv}$ and the normalized waveguide dispersion $v\frac{d^2(v.b)}{dV^2}$ respectively computed by FEM method. The ripples in these figures are due to a limited computational capability of double derivatives terms in waveguide dispersion characteristics. To better represent these graphs we have adopted the higher order polynomial expression scheme which

is discussed in next section. To compute the waveguide dispersion the value of normalized propagation constant should be an accurate enough up to at least 6 decimal points.

4. Modeling of Linearly Chirp Types Refractive Index Profile of Single mode Optical fiber

In this section we will apply our finite element formulation further to estimate the waveguide dispersion for chirped refractive index profile. Now here we define a variety of more complicated than previous case a generalized linear chirp type refractive index profile and is defined as [31-32],

$$n(x) = \begin{cases} n_1 - (n_1 - n_0)\left\{1 + \left|\frac{r}{a}\right| - 1\right\}\exp\left(-\alpha\left|\frac{r}{a}\right|\right)\cos\left\{2\pi N_c\left(\frac{r}{a}\right)^2\right\} & r \le a \\ n_1(1-\Delta) & r > a \end{cases} \qquad (16)$$

where n_1 is the refractive index at the center of the waveguide at $r = 0$, α controls the growth or decay of the profile envelope, N_c is the number of cycles in a core radius, a is the core radius and n_0 is the cladding refractive index. The refractive index profile can be divided into two parameters. One, the fiber parameters like a, n_1, n_0 and other, the profile parameters like α and N_c. By varying these parameters ($a,\ n_0,\ n_1,\ N_c,\ \alpha$), we can generate profiles from simple step index type to complex multiple cladding type as shown in Fig. 9. For an example the profile parameters are $N_c = 0$ and $\alpha = 0$ respectively for step index profile. Figures 10-12 shows the normalized propagation constant b, propagation constant in terms of $\frac{\beta}{k}$ and normalized group delay $\frac{d(v.b)}{dV}$ for the HE_{11} mode of optical fiber having linear chirp types of refractive-index profiles. The waveguide dispersion can be computed straight forward from the Fig. 12 and eq. (15).

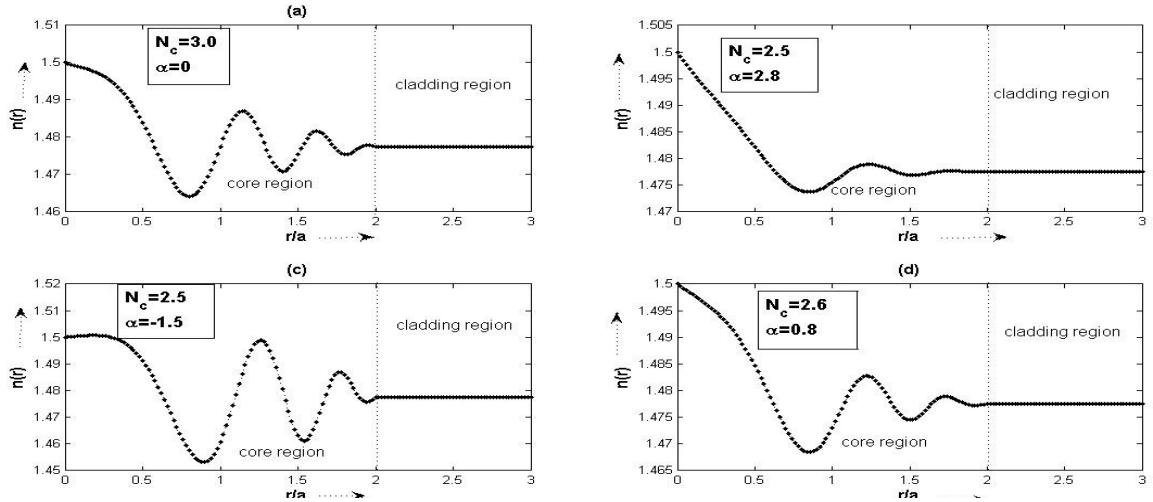

Fig. 9: Various kinds of chirp type refractive index profiles produce by controlling the refractive index profile parameters.

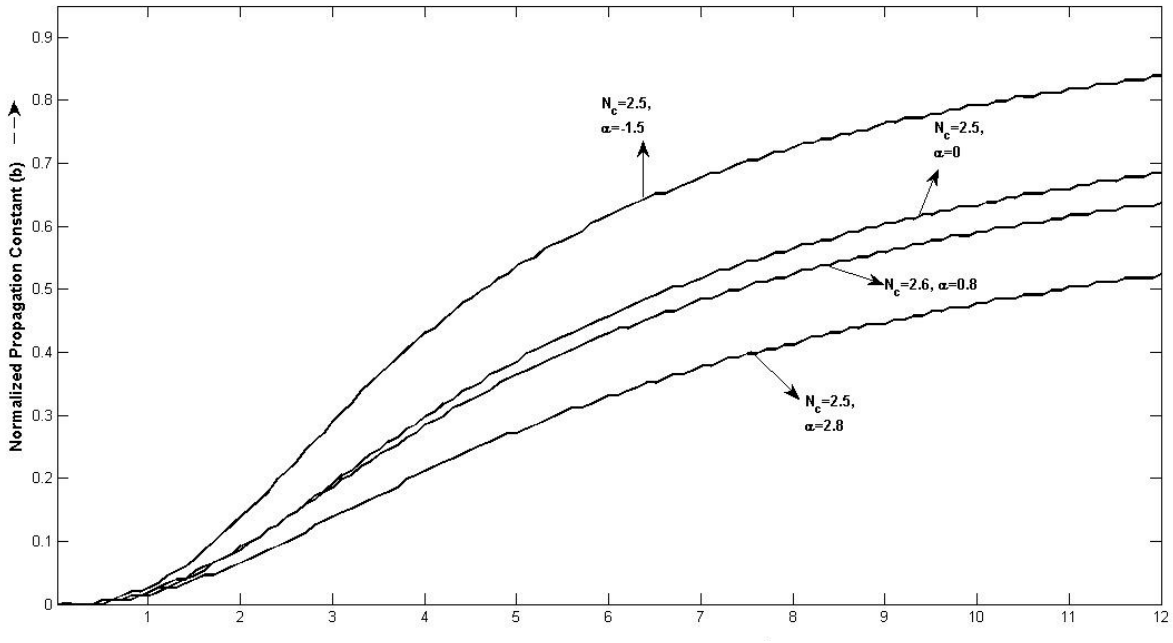

Fig. 10: Normalized propagation constant (b) of optical fiber with linear chirp types of refractive-index profiles.

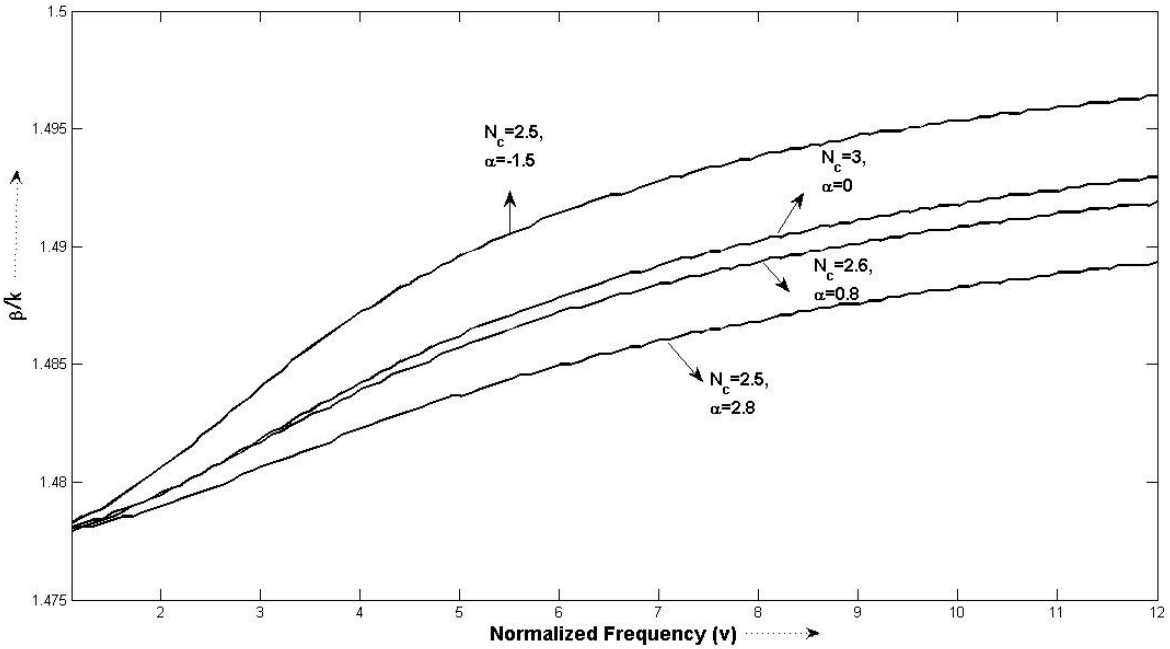

Fig. 11: Propagation constant in terms of $\frac{\beta}{k}$ as a function of v for optical fiber with linear chirp types of refractive index profiles.

It is apparent from the Figures 10-13 that the waveguide dispersion can be substantially reduced, when we deployed the optical waveguide having a complicated refractive index profile. The ripples in the Fig. 12 are due to the limited accuracy of FEM simulation. However this problem can be solved by deriving the appropriate higher order polynomial for Fig. 10 and Fig. 12. In order to obtain the

more accurate results we have derived the higher order polynomial equations, which established the relationship mathematically between b and v-number. Using the described polynomial equations, we can get the similar result and more accurate response of the waveguide dispersion. The polynomial equations, which describe the relation between b and v-number represented in Fig. 4 can be shown by the Table 1.

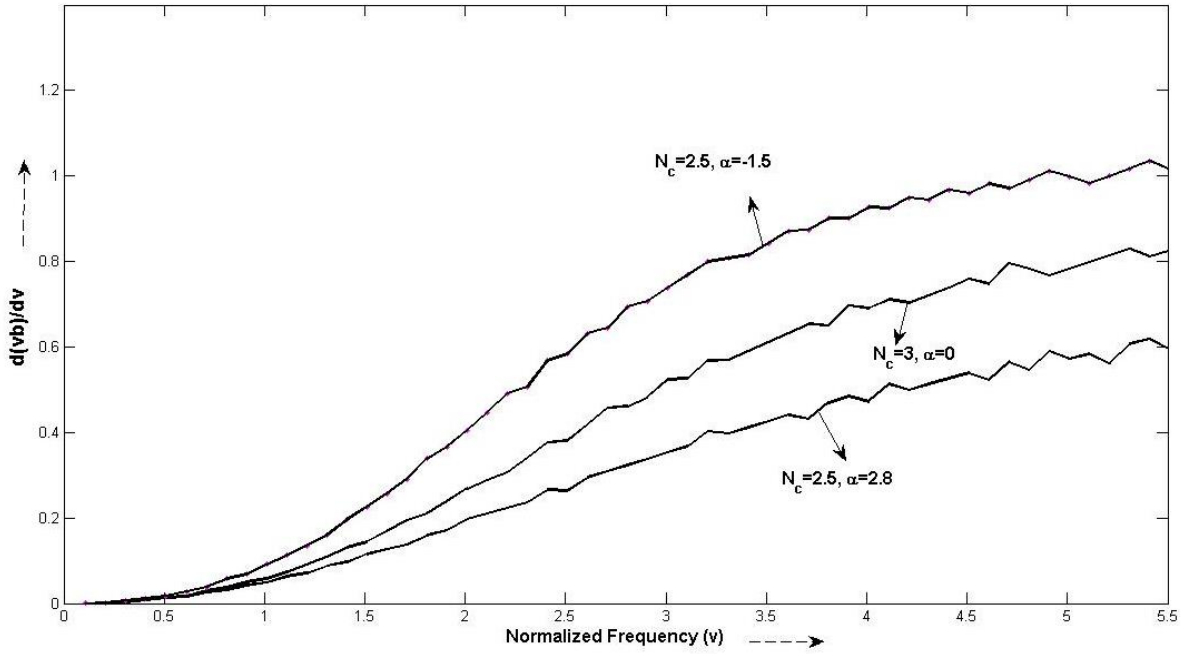

Fig. 12: Normalized delay $\frac{d(Vb)}{dV}$ of optical fiber with linear chirp types of refractive index profile.

Table 1: The Polynomial equation derived for the Fig. 4

<table>
<tr><td>The Value of $(\boldsymbol{\alpha})$</td><td>Derived Polynomial $(\boldsymbol{b\ Vs\ V})$,
$$\boldsymbol{Waveguide\ Dispersion\ (D_W) = -\frac{\frac{(n_1 - n_s)}{c\lambda} V \frac{d^2(Vb)}{dV^2} \times 10^9 ps}{km \times nm}}$$
where $\boldsymbol{c \rightarrow 3 \times 10^5 \frac{km}{sec}, \lambda \rightarrow 1550\ nm}$</td></tr>
<tr><td>1</td><td>$\boldsymbol{b = P_1V^{10} + P_2V^9 + P_3V^8 + P_4V^7 + P_5V^6 + P_6V^5 + P_7V^4 + P_8V^3 + P_9V^2 + P_{10}V + P_{11}}$,
Where
<table>
<tr><th>For optical fiber</th><th>For planar slab waveguide</th></tr>
<tr><td>p1 = -0.00024904
p2 = 0.0049387
p3 = -0.041975
p4 = 0.19927
p5 = -0.57533
p6 = 1.0223
p7 = -1.045
p8 = 0.42761
p9 = 0.19092
p10 = -0.018197
p11 = -8.6465e-00</td><td>p1 = 0.000204
p2 = -0.004029
p3 = 0.033876
p4 = -0.15822
p5 = 0.45012
p6 = -0.81141
p7 = 0.96319
p8 = -0.8419
p9 = 0.6101
p10 = -0.072611
p11 = 0.0010013</td></tr>
</table></td></tr>
<tr><td></td><td>$\boldsymbol{b = P_1V^{10} + P_2V^9 + P_3V^8 + P_4V^7 + P_5V^6 + P_6V^5 + P_7V^4 +}$</td></tr>
</table>

2

$$P_8V^3 + P_9V^2 + P_{10}V + P_{11},$$

Where

For optical fiber	For planar slab waveguide
p1 = -0.00037675	*p1 = 0.00024924*
p2 = 0.007179	*p2 = -0.0052164*
p3 = -0.058293	*p3 = 0.046329*
p4 = 0.26239	*p4 = -0.22793*
p5 = -0.70978	*p5 = 0.6825*
p6 = 1.1518	*p6 = -1.3001*
p7 = -0.98619	*p7 = 1.6465*
p8 = 0.11705	*p8 = -1.514*
p9 = 0.50663	*p9 = 1.0357*
p10 = -0.028838	*p10 = -0.096414*
p11 = -0.00082955	*p11 = 0.00048899*

4

$$b = P_1V^{10} + P_2V^9 + P_3V^8 + P_4V^7 + P_5V^6 + P_6V^5 + P_7V^4 + P_8V^3 + P_9V^2 + P_{10}V + P_{11},$$

For optical fiber	For planar slab waveguide
p1 = -0.00031762	*p1 = -3.6107e-005*
p2 = 0.0065332	*p2 = 0.0010183*
p3 = -0.057385	*p3 = -0.011741*
p4 = 0.28011	*p4 = 0.071828*
p5 = -0.82426	*p5 = -0.25014*
p6 = 1.4626	*p6 = 0.47631*
p7 = -1.399	*p7 = -0.34605*
p8 = 0.32131	*p8 = -0.35521*
p9 = 0.54558	*p9 = 0.78986*
p10 = 0.0070741	*p10 = -0.028264*
p11 = -0.00037985	*p11 = 0.0004006*

8

$$b = P_1V^{10} + P_2V^9 + P_3V^8 + P_4V^7 + P_5V^6 + P_6V^5 + P_7V^4 + P_8V^3 + P_9V^2 + P_{10}V + P_{11},$$

where

For optical fiber	For planar slab waveguide
p1 = 0.000305	*p1 = -0.00021593*
p2 = -0.0060284	*p2 = 0.0043746*
p3 = 0.050768	*p3 = -0.037495*
p4 = -0.23862	*p4 = 0.17534*
p5 = 0.69406	*p5 = -0.47508*
p6 = -1.3341	*p6 = 0.69546*
p7 = 1.8337	*p7 = -0.28413*
p8 = -1.9496	*p8 = -0.70926*
p9 = 1.4209	*p9 = 1.0689*
p10 = -0.078954	*p10 = -0.042595*
p11 = 0.00066221	*p11 = 0.00017185*

100

$$b = P_1V^{10} + P_2V^9 + P_3V^8 + P_4V^7 + P_5V^6 + P_6V^5 + P_7V^4 + P_8V^3 + P_9V^2 + P_{10}V + P_{11},$$

Where

For optical fiber	For planar slab waveguide
p1 = -0.00058377	*p1 = -0.00014847*
p2 = 0.011559	*p2 = 0.0033176*
p3 = -0.096856	*p3 = -0.031052*
p4 = 0.44456	*p4 = 0.15682*
p5 = -1.1997	*p5 = -0.45173*
p6 = 1.8512	*p6 = 0.68015*

	p7 = -1.2765 *p8 = -0.41813* *p9 = 1.1734* *p10 = -0.041564* *p11 = -0.00018982*	*p7 = -0.21595* *p8 = -0.91033* *p9 = 1.2558* *p10 = -0.040894* *p11 = -0.00046561*

On the basis of the polynomial mentioned in table 1, we can obtain the same result represented in the Fig. 4, Fig. 7 and Fig. 8 as shown in the Fig. 13.

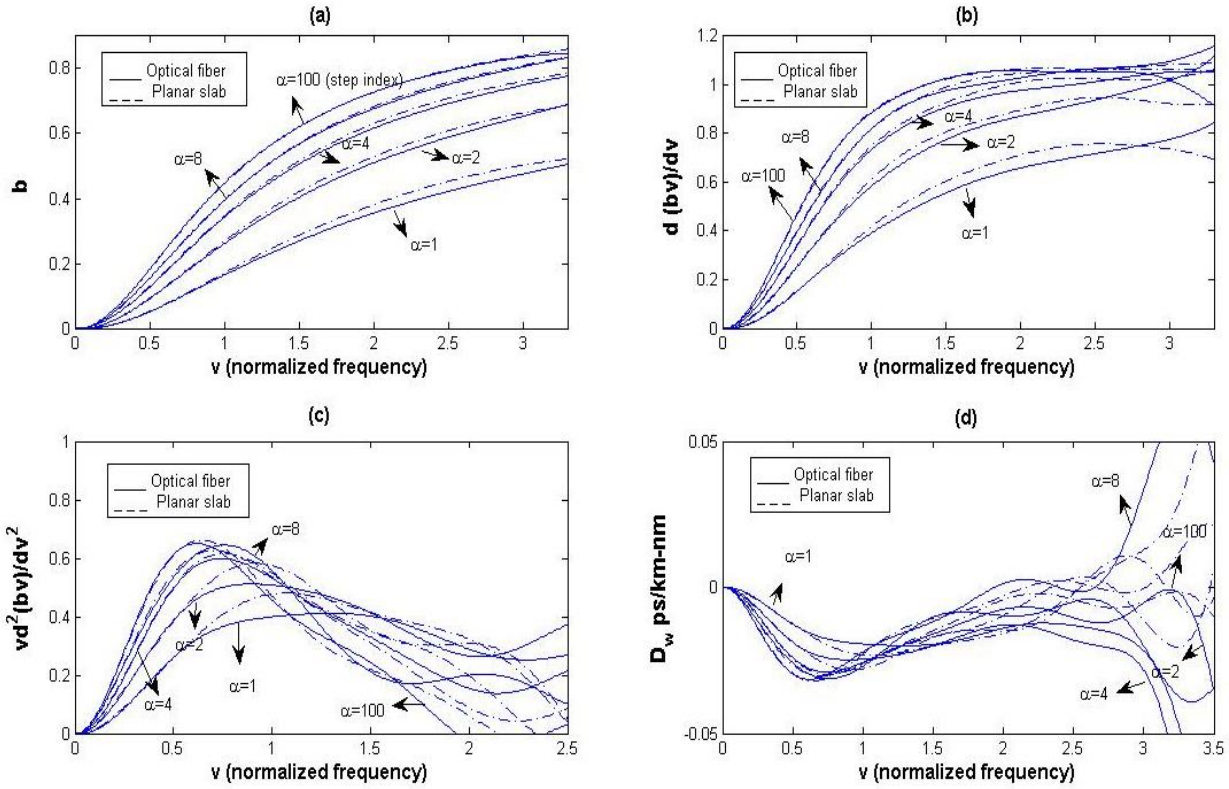

Fig. 13 Simulation result obtained by the derived polynomial represented in the Table 1: (a) b Vs. v-number relation (b) $\frac{d(b.v)}{dv}$ Vs. v- number relation (c) $v\frac{d^2(b.v)}{dv}$ Vs v-number relation (d) Waveguide dispersion for different value of α.

Figure 13 shows that, we are able to obtain the similar results using the derived polynomials represented in the table 1. Fig. 13(a) shows the b versus v-number relation similar to the Fig. 4. On the basis of this, we can calculate the response for $\frac{\mathrm{d(b.v)}}{\mathrm{dv}}$, $\mathrm{v}\frac{\mathrm{d^2(b.v)}}{\mathrm{dv^2}}$ represented in the Fig. 13(b) and 13(c), respectively. Finally, we can calculate the waveguide dispersion, represented in the Fig. 13(d). Hence, this shows that we can consider the derived polynomial as an appropriate mathematical equation for the calculation of the waveguide dispersion. In the same manner, we can show the higher

order polynomial equations, which show the similar result equivalent to the Fig. 10 and Fig. 12. The table 2 shows the derived polynomial equation.

Table 2: The Polynomial equation derived for the Fig. 11

Derived Polynomial ($\boldsymbol{b\ Vs\ V}$)

$$\boldsymbol{Waveguide\ Dispersion\ (D_W) = -\frac{(n_1 - n_s)}{c\lambda} V \frac{d^2(Vb)}{dV^2}}$$

where $\boldsymbol{c \rightarrow 3 \times 10^5 \frac{km}{sec}, \lambda \rightarrow 1550\ nm}$

$$\boldsymbol{b = P_1V^{10} + P_2V^9 + P_3V^8 + P_4V^7 + P_5V^6 + P_6V^5 + P_7V^4 + P_8V^3 + P_9V^2 + P_{10}V + P_{11}},$$

Where, the constant in above relation for various parameter values are

$\boldsymbol{N_c = 2.5,\ \alpha = 0}$	$\boldsymbol{N_c = 2.5,\ \alpha = 2.8}$	$\boldsymbol{N_c = 2.5,\ \alpha = 1.5}$	$\boldsymbol{N_c = 2.5,\ \alpha = 0.8}$
p1 = 1.3805e-009	p1 = 2.1628e-010	p1 = 8.3385e-010	p1 = -1.5755e-009
p2 = -8.7842e-008	p2 = -1.2027e-008	p2 = -4.6045e-008	p2 = 1.2441e-007
p3 = 2.3409e-006	p3 = 2.2808e-007	p3 = 9.5012e-007	p3 = -4.2415e-006
p4 = -3.3688e-005	p4 = -7.5238e-007	p4 = -7.3996e-006	p4 = 8.141e-005
p5 = 0.00028054	p5 = -3.4104e-005	p5 = -2.8064e-005	p5 = -0.00095935
p6 = -0.0013427	p6 = 0.00054423	p6 = 0.00095846	p6 = 0.0070577
p7 = 0.0035993	p7 = -0.0032432	p7 = -0.0069776	p7 = -0.031
p8 = -0.0078156	p8 = 0.0046619	p8 = 0.01881	p8 = 0.068473
p9 = 0.029432	p9 = 0.02717	p9 = 0.0050421	p9 = -0.028334
p10 = -0.0091198	p10 = -0.0096538	p10 = 0.00062066	p10 = 0.013013
p11 = 0.0001478	p11 = 0.00013959	p11 = -0.00065062	p11 = -0.0014513

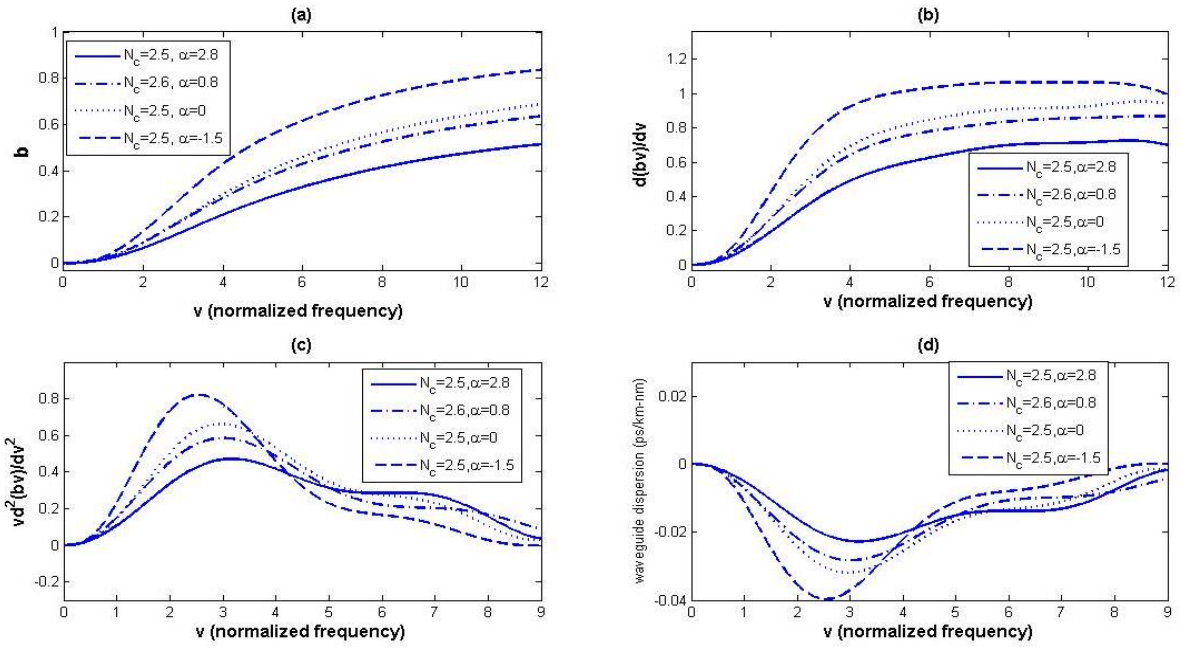

Fig. 14 Simulation result obtained by the derived polynomial represented in the Table 2: (a) b versus v-number relation (b) $\frac{d(b.v)}{dv}$ versus v-number relation (c) $v\frac{d^2(bv)}{dv^2}$ versus v-number (d) Waveguide dispersion for different value of N_c, α .

On the basis of the derived polynomial equations the waveguide dispersion plot can be represented as shown in the Fig. 14 (d). It is apparent while comparing Fig. 13(d) with Fig. 14(d) that in case of complicated chirped type profile case, the waveguide dispersion is flat and negative. Earlier also the profile as shown in Fig. 9 (c), has been analyzed in greater detail for the case of circular core fiber [26]. In literature [26], it has been shown; $\pm 1.5\ ps/km - nm$ waveguide dispersion over the band, but in our case the waveguide dispersion is even smaller as well as flat over the band as reveal in Fig. 14(d). From the Fig. 14(d), it is also apparent that the optimum parameter for lower waveguide dispersion is $N_c = 2.5, \alpha = 1.5$, corresponds to Fig. 9 (c).

5. Conclusion

In the conclusion of the paper, we have characterized the dispersion property of linearly chirp types of refractive index profile. The accuracy of FEM has been tested with respect to the number of core division. We have achieved very good agreement with the previously published results. It has been demonstrated that the numerical error becomes less than 2 % for the number of the core divisions in FEM analyses ≥ 30. Our study also reveals that the optimum chirped type of refractive index profile waveguide can be used to achieve the flat waveguide dispersion property over the band. This study will be useful in optical communication systems where low dispersion link has to be deployed. Commercial software which obeys only the certain geometrical guide-lines, instead our method is flexible to analyze for all type of geometrical shape of holes in the core for photonic crystal fiber. Moreover the accuracy of our FEM method found to be up to 6 decimal points which are sufficient enough to compute the waveguide dispersion and performance is well comparable to commercial software.

Acknowledgment

This work is prepared as part of the post doctorate research work done by Dr. Sanjeev Kumar Raghuwanshi under the project of Erasmus Mundus Scholarship program in a collaboration between City University London, United Kingdom and Indian School of Mines Dhanbad, Jharkhand India. This project has been funded with support from the European Commission. This publication reflects the views only of the author, and the Commission cannot be held responsible for any use which may be made of the information contained therein.

Appendix I

A.1 Derivation of eq. (13)

Since from eq. (5)

$$I(R) = -\int_0^\infty \left(\frac{dR}{d\rho}\right)^2 \rho d\rho + \int_0^\infty [v^2 q(\rho) - w^2] R^2 \rho d\rho \qquad (A.1)$$

We can split the above integration as follow,

$$I(R) = -\int_0^D \left(\frac{dR}{d\rho}\right)^2 \rho d\rho + \int_0^D [v^2 q(\rho) - w^2] R^2 \rho d\rho I(R) - \int_D^\infty \left(\frac{dR}{d\rho}\right)^2 \rho d\rho + \int_D^\infty [v^2 q(\rho) - w^2] R^2 \rho d\rho \qquad (A.2)$$

As we know that

$$R(\rho) = \begin{cases} \sum_{i=0}^{N} R_i \phi_i(\rho) & 0 \le \rho \le D \\ \frac{R_N}{K_0(wD)} K_0(w\rho) & \rho > D \end{cases} \qquad (A.3)$$

Observing the equation (A.1) and (A.2), we can write, since $q(\rho) = 0 \; for \; \rho > D$ hence

$$I(R) = -\int_0^D \left(\frac{dR}{d\rho}\right)^2 \rho d\rho + \int_0^D [v^2 q(\rho) - w^2] R^2 \rho d\rho I(R) - \int_D^\infty \left(\frac{dR}{d\rho}\right)^2 \rho d\rho - \int_D^\infty [w^2] R^2 \rho d\rho \qquad (A.4)$$

Taking the last two term of eq. (A.4) and putting the values of R using equation (A.3), we can write

$$-\int_D^\infty \left[\frac{d}{d\rho}\left(\frac{R_N}{K_0(wD)} K_0(w\rho)\right)\right]^2 \rho d\rho - w^2 \int_D^\infty \left(\frac{R_N}{K_0(wD)} K_0(w\rho)\right)^2 \rho d\rho \qquad (A.4)$$

Since, $\frac{d}{d\rho} K_0(w\rho) = wK_1(w\rho)$, hence we can modify the expression (A.4) as follow

$$-\frac{R_N^2 w^2}{K_0^2(wD)}\left[\int_D^\infty K_1^2(w\rho)\rho d\rho + \int_D^\infty K_0^2(w\rho)\rho d\rho\right] \qquad (A.5)$$

Now Since,

$$\int_a^\infty K_m^2\left\{\frac{w}{a} r\right\} r \, dr = \begin{cases} \frac{a^2}{2}[K_1^2(w) - K_0^2(w)] & m = 0 \\ \frac{a^2}{2}[K_{m-1}(w)K_{m+1}(w) - K_m^2(w)] & m \ge 1 \end{cases} \qquad (A.6)$$

From Eq. (A.5),

$$\int_D^\infty K_1^2(w\rho)\rho d\rho = \int_D^\infty K_1^2\left(\frac{wD}{D}\rho\right)\rho d\rho \qquad (A.7)$$

$$\int_D^\infty K_1^2(w\rho)\rho d\rho = \frac{D^2}{2}[K_0(wD)K_2(wD) - K_1^2(wD)] \quad (A.8)$$

In the same manner,

$$\int_D^\infty K_0^2(w\rho)\rho d\rho = \int_D^\infty K_0^2\left(\frac{wD}{D}\rho\right)\rho d\rho$$

$$\int_D^\infty K_0^2(w\rho)\rho d\rho = \frac{D^2}{2}[K_1^2(wD) - K_0^2(wD)] \quad (A.9)$$

Now putting the values of the expression from eq. (A.8) and (A.9) in eq. (A.5), we get

$$-\frac{R_N^2 w^2}{K_0^2(wD)}\left[\frac{D^2}{2}[K_0(wD)K_2(wD) - K_1^2(wD)] + \frac{D^2}{2}[K_1^2(wD) - K_0^2(wD)]\right]$$

Finally, we can write the above expression,

$$-\frac{R_N^2 w^2 D^2}{K_0^2(wD)}\frac{K_0(wD)}{2}[K_2(wD) - K_0(wD)\,] \quad (A.10)$$

Since we know the identity,

$$\frac{n}{z}K_n(z) = -\frac{1}{2}[K_{n-1}(z) - K_{n+1}(z)] \quad (A.11)$$

From eq. (A.11) and (A.10), we can write,

$$\frac{1}{2}[K_2(wD) - K_0(wD)\,] = \frac{1}{wD}K_1(wD) \quad (A.12)$$

Putting the value, from eq. (A.12) in the eq. (A.10), we can write

$$-\frac{R_N^2 w^2 D^2}{K_0(wD)}\frac{1}{wD}K_1(wD) = -\frac{wDK_1(wD)}{K_0(wD)}R_N^2 \quad (A.13)$$

Hence, we can write,

$$-\int_D^\infty \left[\frac{d}{d\rho}\left(\frac{R_N}{K_0(wD)}K_0(w\rho)\right)\right]^2 \rho d\rho - w^2\int_D^\infty \left(\frac{R_N}{K_0(wD)}K_0(w\rho)\right)^2 \rho d\rho$$

$$= -\frac{wDK_1(wD)}{K_0(wD)}R_N^2 \quad (A.14)$$

Finally, it turns out to be

$$I(R) = -\int_0^D \left(\frac{dR}{d\rho}\right)^2 \rho d\rho + \int_0^D [v^2 q(\rho) - w^2]\,R^2 \rho d\rho I(R) - \frac{wDK_1(wD)}{K_0(wD)}R_N^2 \quad (A.15)$$

A.2 Derivation of eigenvalue equation using stationary condition

The stationary condition of the functional (13) is given by partial differentiation with respect to R_i(i = 0 – N), as

$$\mathbf{0} = \frac{\mathbf{1}}{\mathbf{2}}\frac{\boldsymbol{\delta}\mathbf{I}}{\boldsymbol{\delta}\mathbf{R_i}} = -\int_0^{\mathbf{D}} \frac{\mathbf{dR}}{\mathbf{d\rho}}\frac{\mathbf{d\phi_i}}{\mathbf{d\rho}}\,\boldsymbol{\rho}\mathbf{d\rho} + \mathbf{v^2}\int_0^{\mathbf{D}} \mathbf{q}(\boldsymbol{\rho})\mathbf{R}\boldsymbol{\phi}_\mathbf{i}\boldsymbol{\rho}\mathbf{d\rho} - \mathbf{w^2}\int_0^{\mathbf{D}} \mathbf{R}\boldsymbol{\phi}_\mathbf{i}\boldsymbol{\rho}\mathbf{d\rho} - \frac{\boldsymbol{\omega}\mathbf{D}\mathbf{K_1}(\mathbf{wD})}{\mathbf{K_0}(\mathbf{wD})}\mathbf{R_n}\boldsymbol{\delta}_{\mathbf{i,N}} \qquad (\mathbf{i} = \mathbf{0} - \mathbf{N}) \qquad (\boldsymbol{A}.\mathbf{16})$$

Substituting eq. (11) and eq. (12) in Eq. (A.16) and calculating the stationary conditions in the same way as those in re [12] $(N+1)^{th}$ order simultaneous equations are obtained. In order that Eigen value equations have nontrivial solutions except for $R_0 = R_1 = \cdots = R_N = 0$, the determinant of the matrix C should

$$\boldsymbol{det}(\boldsymbol{C}) = \mathbf{0}. \qquad (\boldsymbol{A}.\mathbf{17})$$

where the matrix elements of C are given by

$$\left.\begin{aligned} c_{0,0} &= \frac{1}{2} - \left(3q_0 + 2q_1\right)\frac{v^2}{60}\,\delta^2 + \frac{w^2}{12}\,\delta^2, \\ c_{i,i} &= 2i - \left[(5i-2)q_{i-1} + 30iq_i + (5i+2)q_{i+1}\right]\frac{v^2}{60}\delta^2 + \frac{2i}{3}\,w^2\delta^2 \quad (i = l - N - 1) \\ c_{i,i+1} = c_{i+1,i} &= -\frac{(2i+1)}{2} - \left[(5i+2)q_i + (5i+3)q_{i+1}\right]\frac{v^2}{60}\delta^2 + \frac{2i+1}{12}\,w^2\delta^2 \quad (i = 0 - N - 1) \\ C_{N,N} &= \frac{2N-1}{2} - \left[(5N-2)q_{N-1} + 3(5N-1)q_N\right]\frac{v^2}{60}\delta^2 + \frac{4N-1}{12}w^2\delta^2 + \frac{wDK_1(wD)}{K_0(wD)}, \end{aligned}\right\} \qquad (A.18)$$

where discretization step δ is given by $\delta = D/N$. When the refractive index distribution $\mathrm{q}(\rho)$ of the fiber and the normalized frequency v are given, the propagation constant β (implicitly contained in w) is calculated from eq. (A.17) and eq. (A. 18).

References

[1]. Zheludev., Nikolay, I.: Photonic-plasmonic devices: a 7-nm light pen makes its mark. Nat. Nanotechnol. 5, 10-11 (2010)

[2]. Politano, A., Chiarello, G.: Quenching of plasmons modes in air-exposed grapheme-Ru contacts for plasmonic devices. Appl. Phy. Lett. 102, 201608 (2013)

[3]. He, X. Y., Wang, Q. J., Yu, S. F.: Numerical study of gain-assisted terahertz hybrid plasmonic waveguide. Plasmonics. 7, 571-577 (2012)

[4]. Baqir, M. A., Choudhary., P. K.: Dispersion characteristics of optical fibers under PEMC twist. Journal of electromagnetic Wave and Application. 28(17) (2014)

[5]. Li, Z.; Bao, K., Fang, Y., Huang, Y., Nordlander, P., Xu, H.: Correlation between incident and emission polarization in nanowire surface plasmons waveguide. Nano. Lett. 10, 1831-1835 (2010)

[6]. Politano. A., Chiarello, G.: Unravelling suitable grapheme-metal contacts for grapheme-based plasmonic device. Nanoscale. 5, 8251-8220 (2013)

[7]. Mussina, R., Selviah, D. R., Fernnandez, F. A., Tijhuis, A. G., Hon, B. P. D.: A rapid accurate technique to calculate the group delay dispersion and dispersion slop of arbitrary radial refractive index profile weakly-guiding optical fibers. Progress in Electromagnetic Research. 145, 99-113 (2014)

[8]. Walpita, L. M.: Solution for planar optical waveguide equation by selecting zero elements in a characteristics matrix. Journal of the Optical Society of America. A2, 592 – 602 (1985)

[9]. Rahman, B. M. A.: Finite element analysis of optical waveguides. Progress in Electromagnetic Research. 10, 187 – 216 (1995)

[10]. Raghuwanshi, S. K., Kumar, A.: A new semi-analytical method for the analysis of tapered optical waveguide. Optik (Elsevier). 125(24), 7515 – 7221 (2014)

[11]. Honkis, T. H.: Analysis of optical waveguide with arbitrary index profile using an immersed interface method. International Journal of Modern Physics C. 22(7), 687 – 710 (2011)

[12]. Okoshi, T., Okamoto, K.: Analysis of wave propagation in inhomogeneous optical fibers using a varational method. IEEE Trans. On Microwave Theory and Tech. MTT-22(11), 938 – 945 (1974)

[13]. Popescu, V. A.: Determination of normalized propagation constant for optical waveguide by using second order variational method. Journal of Optoelectronics and Advanced Mat. 7(5), 2783 – 2786 (2005)

[14]. Rostami, A., Motavali, H.: Asymptotic iteration method: a power approach for analysis of inhomogeneous dielectric slab waveguide. Progress in Electromagnetic Research B. 4, 171-182 (2008)

[15]. Chaudhuri, P. R., Roy, S.: Analysis of arbitrary index profile planar optical waveguide and multilayer nonlinear structure: a simple finite differences algorithm. Opt. Quant. Electron. 39, 221 – 237 (2007)

[16]. Sadiku, M. N. O.: Numerical techniques in electromagnetic: Second Edition CRC Press LLC (1992)

[17]. Booton, R. C.: Computational methods for electromagnetic and microwave. John Wiley and Sons. (1992)

[18]. Kasim, N. M., Mohammad, A. B., Ibrahim, M. H.: Optical waveguide modeling based on scalar finite difference scheme. Journal Teknologi. 45(D), 181-194 (2006)

[19]. Gambling, W. A., Payne, D. N., Matsumura, H.: Cut-off frequency in radically inhomogeneous single mode fiber. Electron. Letters. 13(5), 130 – 140 (1977)

[20]. Zhuangqi, C., Jiang, Y., Yingli, C.: Analytical investigation of planar optical waveguide with arbitrary index profiles. Optical and Quant. Electronics. 31, 637 – 644 (1999)

[21]. Chiang, K. S.: Review of numerical and approximation methods for modal analysis of general dielectric waveguide. Opt. Quantum Electron. 26, 113 – 134 (1994)

[22]. Xu, W., Wang, Z. H., Huang, Z. M.: Propagation constant of a planar dielectric waveguide with arbitrary refractive index variation. Opt. Lett. 18, 805 – 807 (1993)

[23]. Okamoto, K.: Fundamentals of optical waveguide. Academic Press (2006)

[24]. Sharma, E. K., Goyal, I. C., Ghatak, A. K.: Calculation of cut-off frequencies in optical fibers for arbitrary profiles using the matrix method. IEEE Journal of Quant. Electron. QE-17(12), 2317 – 2320 (1981)

[25]. Okamoto, K., Okoshi, T.: Analysis of wave propagation in optical fibers having core with α-power refractive distribution and uniform cladding. IEEE Trans. On Microwave Theory and Tech. MTT-24(7), 416 – 421 (1976)

[26]. Raghuwanshi, S. K., Kumar, S.: Analytical expression for dispersion properties of circular core dielectric waveguide without computing $d^2\beta/dk^2$ numerically. I-manager's Journal on Future engineering & Technology. 7(3), 26-34 (2012)

[27]. Ghatak, A. K., Thyagarajan, K.: Optical electronics: introduction to fiber optics. Cambridge Press (1999)

[28]. Hotate, K. A., Okoshi, T.: Formula giving single-mode limit of optical fiber having arbitrary refractive index profile. Electron. Letters. 14(8), 246 – 248 (1978)

[29]. Rostami, A., Moyaedi, S. K.: Exact solution for the TM mode in inhomogeneous slab waveguides. Laser Physics. 14(12), 1492 – 1498 (2004)

[30]. Survaiya, S. P., Shevagaonkar, R. K.: Dispersion characteristics of an optical fiber having linear chirp refractive index profile. IEEE Journal of Lightwave Tech. 17(10), 1797 – 1805 (1999)

[31]. Raghuwanshi, S. K., Talabattula, S.: Dispersion and peak reflectivity analysis in a non-uniform FBG based sensors due to arbitrary refractive index profile. Progress in Electromagnetic Research B. 36, 249-265 (2012).

[32]. S. K. Raghuwanshi, and B. M. A. Rahman "Analysis of Novel Chirped Types of Refractive Index Profile Metamaterial Planar Slab Optical Waveguide by Finite Element Method for Sensor Application" *IEEE Sensor Journal,* vol. 15, no. 7.pp. 4141-4147, 2015

[33]. Sanjeev Kumar Raghuwanshi, and B. M. Azizur Rahman, "Propagation and Characterization of Novel Graded and Linearly Chirped Type's of Refractive Index Profile Symmetric Planar Slab waveguide by Numerical Means", *Progress in Electromagnetic Research-B* (MIT-USA), vol. 62, pp. 255-275, 2015.

[34]. Sanjeev Kumar Raghuwanshi, Santosh Kumar,Ajay Kumar "Dispersion characteristics of complex refractive-index planar slab optical waveguide by using finite element method" *Optik (Elsevier),*Vol. 125 (20), pp. 5929-5935, Oct 2014